

# A Gain-of-Function Mutation of the *SCN5A* Gene Causes Exercise-induced Polymorphic Ventricular Arrhythmias

*Swan et al. SCN5A Mutation Causing Exercise-Induced Polymorphic Tachycardia*

Heikki Swan, MD, PhD\*, Mohamed Yassine Amarouch, PhD<sup>†</sup>, Jaakko Leinonen, MSc<sup>‡</sup>, Annukka Marjamaa, MD, PhD\*, Jan P. Kucera, MD<sup>§</sup>, Päivi J. Laitinen-Forsblom, PhD<sup>||</sup>, Annukka M. Lahtinen, PhD<sup>||</sup>, Aarno Palotie<sup>‡</sup>, MD, PhD, Kimmo Kontula, MD, PhD<sup>||</sup>, Lauri Toivonen, MD, PhD\*, Hugues Abriel, MD, PhD<sup>†</sup>, Elisabeth Widen, MD, PhD<sup>‡</sup>

\*Heart and Lung Center, Helsinki University Central Hospital, Helsinki, Finland, <sup>†</sup>Department of Clinical Research, University of Bern, Bern, Switzerland, <sup>‡</sup> Institute for Molecular Medicine Finland (FIMM), University of Helsinki, Helsinki, Finland, <sup>§</sup>Department of Physiology, University of Bern, Bern, Switzerland, <sup>||</sup> Department of Medicine, University of Helsinki and Helsinki University Central Hospital, Helsinki, Finland

## Correspondence

Dr. Heikki Swan, MD, PhD

Helsinki University Hospital

Heart and Lung Center

P.O. BOX 340

FIN-00029 Helsinki, FINLAND

telephone +358 - 9 - 4717 2442 fax +358 - 9 - 4717 4574

e-mail [heikki.swan@helsinki.fi](mailto:heikki.swan@helsinki.fi)

Word count : 7471

## **Abstract**

**Background.** Over the past 15 years, a myriad of mutations in genes encoding cardiac ion channels and ion channel interacting proteins have been linked to a long list of inherited atrial and ventricular arrhythmias. The purpose of this study was to identify the genetic and functional determinants underlying exercise-induced polymorphic ventricular arrhythmia present in a large multi-generational family.

**Methods and Results.** A large 4-generation family presenting with exercise-induced polymorphic ventricular arrhythmia, which was followed for 10 years, was clinically characterized. A novel *SCN5A* mutation was identified via whole-exome sequencing and further functionally evaluated by patch-clamp studies using HEK293 cells. Of 37 living family-members, a total of 13 individuals demonstrated 50 or more multiformic premature ventricular complexes or ventricular tachycardia upon exercise stress tests when sinus rate exceeded  $99 \pm 17$  beats per minute. Sudden cardiac arrest occurred in one individual during follow-up. Exome-sequencing identified a novel missense mutation (p.I141V) in a highly conserved region of the *SCN5A* gene, encoding the Na<sub>v</sub>1.5 sodium channel protein that co-segregated with the arrhythmia phenotype. The mutation p.I141V shifted the activation curve toward more negative potentials and increased the window current, while action potential simulations suggested that it lowered the excitability threshold of cardiac cells.

**Conclusions.** Gain-of-function of Na<sub>v</sub>1.5 may cause familial forms of exercise-induced polymorphic ventricular arrhythmias.

Key words: tachycardia, ventricular; clinical genetics; *SCN5A*; mutation;

Since 1995, a myriad of mutations in the genes coding for cardiac ion channel subunits or proteins interacting with ion channels were described in patients with inherited forms of arrhythmic disorders such as congenital long QT syndrome (LQTS), Brugada syndrome (BrS) and catecholaminergic polymorphic ventricular tachycardia (CPVT), hence defining cardiac genetic channelopathies. Most of these disorders have demonstrated a broad genetic and phenotypic heterogeneity. *SCN5A* is the gene encoding the pore-forming subunit, Na<sub>v</sub>1.5, mediating the Na<sup>+</sup> current (I<sub>Na</sub>) of cardiac cells. The arrhythmic phenotypes linked to the mutations in *SCN5A* are variable including LQTS type 3, BrS, many forms of conduction defects, atrial fibrillation, sudden infant death syndrome, and dilated cardiomyopathy<sup>1</sup>. More recently, three studies<sup>2,3,4</sup> have reported on a new *SCN5A*-dependent clinical presentation called multifocal ectopic Purkinje-related premature contractions (MEPPC) caused by the mutation p.R222Q.

Premature ventricular complexes (PVCs) emerging at rest in a structurally normal heart are usually considered harmless<sup>5</sup> whereas PVCs provoked by sympathetic stimulus, such as physical exercise, are regarded as significant finding, necessitating further evaluation. In a proportion of cases, PVCs indicate a risk for lethal ventricular tachycardia or fibrillation. Exercise-induced PVCs, bigeminy and ventricular tachycardias in structurally normal hearts, characteristic for CPVT, associate with considerable mortality<sup>6-8</sup>. In fact, lethal arrhythmias may occur in CPVT even before diagnostic exercise-induced symptoms can be verified<sup>9</sup>.

The purpose of this study was to identify the genetic and functional determinants underlying exercise-induced polymorphic ventricular arrhythmia present in a large multigenerational family. Using whole exome-sequencing, a novel *SCN5A* mutation with strong co-segregation with the symptomatic patients was found. Functional and computational studies suggest that the mutation-induced biophysical alterations lead to atrial, Purkinje cells, and ventricular hyperexcitability. These findings further expand the spectrum of cardiac arrhythmias caused by *SCN5A* variants.

## **METHODS**

A Finnish family with 37 living members in four generations was evaluated (**Fig. 1**). Altogether 31 family members underwent cardiological examination, including electrocardiographic tests and cardiac ultrasonography between years 2002 and 2003. In 2013, at the end of the follow-up period, all family members were recontacted and invited for assessment of their symptoms and possible cardiovascular interventions. Informed consent was obtained from all patients. The study was carried out in accordance with the Helsinki Declaration and was approved by the local ethical review board.

### **Electrocardiographic and ultrasonographic examinations**

Standard electrocardiogram (ECG) was recorded at rest (50 mm/s, 0.1 mV/mm). QT interval was measured from lead II and adjusted for heart rate (QTc) according to the Fridericia's correction formula. Bicycle ergometer test was performed with continuous 12-lead ECG recording. The initial load was 30 W, followed by increments of 15 W each minute. The total number of PVCs and the maximum number of consecutive PVCs in ventricular salvos were counted during work phase.

A 24-hour ambulatory ECG was recorded on an out-patient basis. Rhythm, mean heart rate, number of ventricular premature complexes and number and maximum length of ventricular tachycardias ( $\geq 3$  consecutive ventricular complexes) were calculated. Echocardiography was performed using parasternal long- and short-axis and apical 4-chamber views. Aortic root dimension was measured at the sinus valsalva level. Left ventricular dimensions and wall thickness were measured from the M-mode recordings. Doppler echocardiography was used to exclude any valvular stenosis or regurgitation.

## Phenotypic classification of family members

Patients with  $\geq 50$  polymorphic PVCs or  $>10$  polymorphic PVCs per minute or ventricular tachycardia during exercise stress test (ET) were considered affected. Individuals who were unable to perform an exercise stress test were classified as unknown.

## Sequencing of candidate genes

Mutations in *RYR2* were excluded by sequencing its all translated exons and exon-intron boundaries in the DNA sample of the proband (AMC, University of Amsterdam, Netherlands).

Whole-exome sequencing of eight affected pedigree-members was carried out using the NimbleGen SeqCapEZ sequence capture technology ([www.nimblegen.com/products/seqcap/ez/index.html](http://www.nimblegen.com/products/seqcap/ez/index.html)). The exome targets of the patients' DNA were captured with the NimbleGen SeqCap Ez Human Exome Library v2.0, followed by sequencing with the Illumina Genome Analyzer-IIx platform at the Technology Center at the Institute for Molecular Medicine Finland (FIMM). The alignment to human reference genome hg19 and variant calling of chromosomal regions with a sequence-coverage of at least 9x was carried out using the variant calling pipeline of the Institute for Molecular Medicine Finland (FIMM)<sup>10</sup>. The data were filtered to capture only rare coding variants, i.e. variants giving rise to missense, nonsense, splice site or frame shift mutations either with minor allele frequencies  $<0.005$  or not at all present in the 1,000 genomes catalogue of human genetic variation (<http://browser.1000genomes.org/index.html>). The presence of a chr3:38,663,952 T->C variant in the *SCN5A* gene, initially identified by exome sequencing, was assessed in all affected and unaffected family-members by direct Sanger sequencing using forward primer 5'TACTCACTCGACATACTTGG 3' and reverse primer 5'CTTGGAGACCCTGTTTATTG 3'. The sequencing reactions were run on an Applied Biosystems 96-capillary 3730xl DNA Analyzer and analyzed with the Variant Reporter software (Applied Biosystems, US) at the Technology Center at the Institute for Molecular Medicine Finland

(FIMM). The predicted impact of the rare coding *SCN5A* variant identified was analyzed by PolyPhen2 (<http://genetics.bwh.harvard.edu/pph2/>) and SIFT (<http://sift.jcvi.org/>) .

### **Microsatellite genotyping**

Genome-wide linkage mapping was carried out using ABI PRISM Linkage mapping Set MD10 (Applied Biosystems). Standard PCR-protocols were used for amplification of microsatellite fragments using 10 ng of genomic DNA as a template. The fluorescently labelled PCR products were separated using ABI3730 (Applied Biosystems) automated electrophoresis system and the genotype calls were made using GeneMapper3.7 software. Two independent reviewers verified all allele calls, and any discrepancies were resolved. Genotypes were checked for violation of Mendelian segregation of alleles using PEDCHECK<sup>11</sup>

### **Linkage analysis**

Linkage analysis using exercise-induced frequent polymorphic ventricular premature complexes during an exercise test as a dichotomized trait was carried out using the program Merlin (<http://www.sph.umich.edu/csg/abecasis/merlin/index.html>). The analyses were run applying an affected only approach in which the phenotype of all unaffected family-members was assumed be unknown, and the disease allele frequency was set to 0.0001.

### **Site-directed mutagenesis**

Site-directed mutagenesis was performed on pCDN3.1-hSCN5A using the Quick-Change II XL site-directed mutagenesis kit (Stratagene) according to the manufacturer's instructions. The construct was completely sequenced to ensure that there was no other mutation present.

## **Cell culture**

Human Embryonic Kidney 293 cells (HEK293) were cultured at 37°C in Dulbecco's Modified Eagle Medium (DMEM) supplemented with 10% (Fetal bovine serum) FBS, 4 mM glutamine, and 20 mg/ml gentamicin in a humidified atmosphere of 5% CO<sub>2</sub> and 95% air. All cell medium components, except glutamine (Sigma-Aldrich), were purchased from Gibco.

## **Cellular electrophysiology**

The HEK293 cells were transfected with DNA complexed to JetPEI (Polyplus-transfection) according to the manufacturer's instructions. DNA concentrations were 1 µg of pCDN3.1- Na<sub>v</sub>1.5 wild type (WT), p.I137V or p.I141V and 1 µg of pIRES-hβ1-CD8. The resulting Na<sub>v</sub>1.5 protein is a splice variant lacking a glutamine at position 1077 (Q1077del). Eight hours after transfection, the cells were isolated and seeded in plastic Petri dishes at low density. Twenty four hours after transfection, the resulting sodium current ( $I_{Na}$ ) was recorded at room temperature (23-25 °C), under whole-cell voltage clamp conditions with an Axopatch 200B (Axon Instruments, Inc) amplifier interfaced to a personal computer and driven by the PClamp 10 software (Molecular Devices Corporation). Capacitance and series resistances were compensated (60-80% compensation), and the residual capacitive currents were cancelled using a P/4 protocol. The cells were bathed with an extracellular solution containing (in mmol/L): NaCl 50, NMDG-Cl 80, CsCl 5, MgCl<sub>2</sub> 1.2, CaCl<sub>2</sub> 2, HEPES 10, glucose 5. The pH was adjusted to 7.4 with CsOH. Glass pipettes (tip resistance: 1.5 to 3 MΩ) were filled with an intracellular medium containing (in mmol/L): CsCl 60, aspartic acid 50, CaCl<sub>2</sub> 1, MgCl<sub>2</sub> 1, HEPES 10, EGTA 11, Na<sub>2</sub>ATP 5. pH was adjusted to 7.2 with CsOH. For the window current measurements, the presented recordings are normalized to the peak current obtained at -20 mV and are tetrodotoxin (TTX)-subtracted (30 µM).

All products were purchased from Sigma, except TTX, which was obtained from Alomone.

## Computer simulations of $I_{Na}$ , action potentials and conduction

The  $I_{Na}$  and action potentials were simulated using the ten Tusscher-Noble-Noble-Panfilov (TNNP) human ventricular cell model<sup>12</sup> the Courtemanche-Ramirez-Nattel human atrial cell model (CRN)<sup>13</sup>, and the Stewart-Aslanidi-Noble-Noble-Boyett-Zhang (SANNBZ) Purkinje cell model<sup>14</sup>. In all three models,  $I_{Na}$  is represented according to a Hodgkin-Huxley formalism,  $I_{Na} = gNa_{max} m^3 h j (V_m - E_{Na})$ , where  $gNa_{max}$  is the maximal conductance of  $I_{Na}$ ,  $m^3$  represents three activation gates,  $h$  and  $j$  are inactivation gates,  $V_m$  is the membrane potential, and  $E_{Na}$  is the Nernst potential of sodium. The  $I_{Na}$  formulation in the TNNP and SANNBZ models, which are based on human  $I_{Na}$  recordings are equivalent up to the maximal conductance of  $I_{Na}$ , but they differ in terms of steady state values and time constants of the different gates from the  $I_{Na}$  formulation in the CRN model, which is based on that of Luo and Rudy<sup>15</sup>. Table 3 presents the modifications of  $I_{Na}$  that were introduced in the three models to match the experimental data.

Action potential propagation was simulated in a 1 cm long fiber based on the equation

$$\partial V_m / \partial t = -I_{ion} + D \partial^2 V_m / \partial x^2,$$

where  $I_{ion}$  is the sum of the ionic currents normalized to cell capacitance and  $D$  is the diffusion constant, which depends on intra- and intercellular conductance and surface-to-volume ratio. For all three models,  $D$  was set to  $0.00154 \text{ cm}^2/\text{ms}$  as in the original TNNP model<sup>12, 16</sup>, which corresponds to the normal level of gap junctional coupling in the direction of myocardial fibers. Using the same  $D$  allows a direct comparison of conduction between the three models. Gating variables were integrated using the method of Rush and Larsen and the other model variables using the forward Euler algorithm, with  $\Delta x = 0.01 \text{ cm}$  and  $\Delta t = 0.005 \text{ ms}$ . The fiber was stimulated at one extremity and conduction velocity was computed using linear regression of activation times (occurrence of  $dV/dt_{max}$ ) over a segment extending from 25% to 75%

of fiber length. Of note, the computer simulations have the limitation that the models did not incorporate the effects of adrenergic stimulation. Of note, in the current study, we did not incorporate any variability in the computer simulations. All the used values are the arithmetic means of the given parameters.

### **Data analysis and statistical methods**

Currents were analyzed with Clampfit software (Axon Instruments, Inc). Data were analyzed using a combination of pClamp10, Excel (Microsoft) and Prism (graphpad).

Comparisons between groups were performed with two-tailed Student's *t* test or ANOVA for normally distributed parameters. The Kolmogorov-Smirnov test was used to test the normality of the analyzed experimental data. Data are expressed as mean  $\pm$  SD. A p-value <0.05 was considered significant.

## RESULTS

The structure of the Finnish family segregating the exercise-induced arrhythmia syndrome is shown in **Fig. 1A** and the findings of the electrocardiographic and cardiac ultrasonography studies are presented in **Table 1**. Of those alive in the four-generation family, a total of six individuals had experienced a syncopal spell. One case of sudden cardiac death occurred during prospective follow-up. Family member II-1 had died at the age of 2 years. None of the family members had a documented coronary artery disease or a history of angina pectoris.

### ECG registrations

Of sixteen adult  $\text{Na}_v1.5$  p.I141V mutation carriers, five presented with sinus rhythm, one with atrial flutter, and 11 with ectopic atrial rhythm in their resting ECG (**Table 1**, **Fig. 2A** and **Fig. 2B**). Nodal escape rhythm was seen occasionally (**Fig. 2C**). PVCs were not present in resting ECG in any of the family members at first examination. The sinus rate at rest was higher in  $\text{Na}_v1.5$  p.I141V mutation carriers than in non-carriers (**Table 2**). PQ- and  $\text{QT}_{\text{tc}}$  -intervals, QRS -complex morphology and duration, ST segment and T-wave pattern were normal in all during sinus rhythm.

A total of 32 subjects were studied by repeated ETs. The first ET showed 50 or more PVCs during exercise in ten and the subsequent ETs revealed the same in three additional individuals, all carriers of  $\text{Na}_v1.5$  p.I141V mutation. During the ETs, the ventricular arrhythmias progressively became more complex and abundant in parallel with the increasing sinus rate; examples are shown in **Fig. 2D, 2E**. Some of the QRS complexes show varying morphology. In nine out of thirteen ET positive subjects arrhythmia progressed to non-sustained polymorphic ventricular tachycardia ( $\geq 3$  successive complexes, **Fig. 2F**). The average sinus rate at which the ventricular arrhythmias initially appeared was  $99 \pm 17$  beats per minute, and arrhythmias disappeared rapidly after discontinuation of

exercise. The maximum sinus rate achieved during exercise was on average  $97 \pm 8$  % of the age-specific maximum.

### **Cardiac ultrasonography**

In cardiac ultrasonography, all  $\text{Na}_v1.5$  p.I141V mutation carriers showed normal left ventricular end-diastolic diameter and index ( $48 \pm 3$  mm and  $24.5 \pm 2.8$  mm/m<sup>2</sup>, respectively). Aortic root diameter was  $\geq 44$  mm in three of them.

### **Detection of the *SCN5A* mutation**

By using whole exome-sequencing we detected a novel missense mutation, (chr3:38,663,952 T->C) in *SCN5A*, encoding for the  $\text{Na}_v1.5$  sodium channel protein, in addition to two rare coding mutations i.e. rs148604148 (missense, MAF 0.002) in *XYLB*, encoding for xylulokinase homolog (*H. influenzae*) and rs141040660 (synonymous, MAF 0.0005) in *ANO10*, encoding for anoctamin 10, that were shared by all 8 sequenced individuals. The three genes are located at 5 Mb distance from each other on chromosome 3p22.2, but only *SCN5A* is expressed in cardiac tissue and is known to be associated with several arrhythmia disorders, including congenital LQTS type 3, BrS, and idiopathic ventricular fibrillation.

Because the exome sequencing resulted in low coverage across chr3:38,663,952, i.e. 3x to 9x, the initial analyses showed the presence of the chr3:38,663,952 T->C variant in 7 out of 8 analyzed affected family-members. Nonetheless, targeted sequencing of the complete family showed that all 13 affected pedigree-members in addition to 4 unaffected family-members and 3 children with unknown phenotype carried the chr3:38,663,952 T->C mutation (representative sequence traces from four family members are presented in **Fig. 1B**). Based on PolyPhen2- and SIFT-analyses, the mutation, which results in an isoleucine to valine substitution at position 141 of the  $\text{Na}_v1.5$  protein (p.I141V), was classified as possibly damaging with a score of 0.46 and deleterious with a score of 0.00, respectively. Moreover, the mutation

appears to be unique to this family. It is not present in the published 1,000 genomes dataset, of which 83 are Finnish subjects, neither was it present in exome sequence data from 580 unrelated Finnish subjects (unpublished observation), further indicating that this sequence variant is rare. Finally, we performed linkage analyses to assess the probability that all affected individuals share a mutation. The chr3:38,663,952 T->C variant yielded a 2-point LOD-score of 3.56 (conservatively classifying only individuals with >50 exercise-induced polymorphic complexes as affected), whereas genome-wide linkage analyses of the whole pedigree utilizing microsatellite genotypes indicated that the chr3:38,663,952 T->C variant resided in the only chromosomal region displaying complete co-segregation with the arrhythmia phenotype. No mutations were found in the genes *RYR2* and *CASQ2*.

#### **Effects of p.I141V mutation on Na<sub>v</sub>1.5 channel function in HEK293 cells**

To investigate the functional consequences of the p.I141V mutation on the Na<sup>+</sup> channel activity, we used the whole-cell configuration of the patch-clamp technique. The presence of the mutation did not modify the Na<sup>+</sup> current density (**Online Table 1A**). The voltage-dependence of steady state activation was shifted towards more negative potentials (-7 mV) in the presence of the mutation (p<0.01, **Fig. 3A, Fig. 3B, Online Table 1A**). For a given command voltage, the activation and inactivation kinetics were accelerated in the mutant channel (**Fig. 3C and Fig. 3D**). However, no significant differences were observed regarding the voltage dependence of steady state inactivation (**Fig. 3B, Online Table 1A**), the recovery from fast inactivation (**Fig. 3E**), and the onset and recovery from slow inactivation (**Online Fig. 1A, Online Fig. 1B**).

Based on the negative shift of the steady state activation curve, we predicted an increase of the window sodium current (**Fig. 3B inset**). To investigate this window current, we examined the responses of cells transfected with Na<sub>v</sub>1.5 WT and p.I141V channels to a ramp voltage protocol, in which membrane potential was gradually changed between -100 and +50 mV at 0.5 mV/ms. Compared to the

WT window current, the p.I141V window current exhibited a larger peak and this peak was shifted towards more negative potentials (**Fig. 3F, Online Fig. 1C, Online Fig. 1D**).

### **The importance of the p.I141 residue on Na<sub>v</sub>1.5 channel function**

The isoleucine 141 (I141) amino acid is highly conserved across species and voltage gated sodium channels isoforms (**Fig. 1C, Fig. 1D**). The importance of the p.I141 position on Na<sub>v</sub>1.5 function was investigated by mutating the nearest and highly conserved isoleucine 137 to valine. Interestingly, this particular substitution (p.I137V) did not modify any of the Na<sub>v</sub>1.5 channel properties investigated (**Online Fig. 2**).

### **Atrial, ventricular, and Purkinje cell action potential (AP) and conduction modelling**

To investigate the functional consequences of the cardiac hyperexcitability due to the p.I141V mutation of Na<sub>v</sub>1.5, we incorporated the p.I141V Na<sub>v</sub>1.5 properties observed experimentally into the atrial CRN, the ventricular TNNP, and the Purkinje SANNBZ cell models. The I<sub>Na</sub> formulations in all models were modified to reproduce the biophysical changes due to the p.I141V mutation (see Methods and **Fig. 4A-C**). In the I<sub>Na</sub> formulations of all models, the effects of the p.I141V mutation were simulated by shifting the voltage dependence of the steady state equilibrium  $m_{\infty}$  and the time constant  $\tau_m$  of the  $m$  gates by an equal amount to recapitulate the shift of the steady state activation curve and the acceleration of activation, and by shifting the voltage dependence of the closing rate constant  $\beta_h$  of the  $h$  gate to recapitulate the acceleration of fast inactivation with no change in the recovery from inactivation. The  $j$  gate was left unchanged. The formulations used are summarized in **Table 3**.

Simulations were run using the three cell models for WT, using both heterozygous and homozygous p.I141V genotypes, and strength-duration curves were constructed. In the three models, a lower excitation threshold for AP generation (pacing rates: 1 Hz and 2.5 Hz for the atrial and ventricular

models, 2.5 Hz for the Purkinje model) was observed in the homozygous and heterozygous p.I141V genotypes compared to the WT (**Fig. 4D-I**) Interestingly, at both pacing rates, the strength-duration curve for the heterozygous genotype was very close to the curve for the homozygous genotype. In the Purkinje cell model, we observed that the p.I141V mutation accelerates the rate of spontaneous activity, even in the heterozygous state (**Inset Fig. 4F**).

Conduction velocity was investigated in fibers of CRN, TNNP, and SNNBZ cell models (pacing rates: as described above). As shown in **Fig. 4J-L**, the presence of the p.I141V mutation in homozygous and heterozygous states accelerated atrial and ventricular conduction in a similar manner at 1 Hz and 2.5 Hz, and it accelerated conduction in the Purkinje fiber at 2.5 Hz.

### **Clinical follow-up**

During a follow-up of 10 years, altogether 38% of 16 adult  $Na_v1.5$  p.I141V carriers have either permanent (n=4) or paroxysmal (n=2) atrial fibrillation. At the end of the follow-up period, beta-antiadrenergic medication was used by ten individuals, one of whom was also using amiodarone. An implantable defibrillator (ICD) was implanted in another tertiary care center to one family member (II:14) due to non-sustained ventricular tachycardias. Left ventricular dilatation or systolic heart failure was detected in none of the family members during follow-up. The dilated aortic root had not required surgical intervention in any of the cases during follow-up.

Another family member (III-3) died during the follow-up 3 years after a mitral valve replacement. He had been followed from the age of 36 due to frequent multiformic premature ventricular complexes, paroxysmal atrial fibrillation and mitral valve prolapse. Perioperative pulmonary vein isolation was unsuccessful in eliminating AF. A ventricular pacemaker was implanted and AV-nodal ablation was performed resulting in temporary AV block. During follow-up, the patient experienced a syncopal spell

three times. A month later sudden cardiac arrest occurred at home during stressful conditions; patient was resuscitated from ventricular fibrillation but died few days later.

Additionally, we repeated exercise stress tests to all family-members (n = 21, including both mutation carriers and family-members not carrying the Na<sub>v</sub>1.5 p.I141V mutation) whose exercise stress test was normal at the first examination. In the follow-up test, three individuals (V-7, III-11, and II-7) showed 50 or more PVCs at the age of 31, 45 and 69 years, respectively. They were all carrying the Na<sub>v</sub>1.5 p.I141V mutation.

The ambulatory 24-hour ECG recording was performed at the end of follow-up period in 14 Na<sub>v</sub>1.5 p.I141V mutation carriers to assess the burden of AF. This revealed one additional patient (II:14) with AF which would not have been diagnosed during exercise stress tests. At resting heart rates, PVCs were absent or their frequency was low in most Na<sub>v</sub>1.5 p.I141V mutation carriers but their incidence increased concomitantly with physical activity and increasing sinus rate as illustrated in **Online Fig 3**.

## DISCUSSION

In the present study, we describe a novel missense mutation in a highly conserved region of the *SCN5A* gene, which associates with an autosomal dominantly inherited arrhythmic phenotype in a large multigenerational Finnish family. This phenotype, which is characterized by polymorphic PVCs, bigeminy and non-sustained polymorphic ventricular tachycardia, provoked by physical exercise and disappearing after cessation of exercise in structurally normal hearts.

The affected family members displayed widespread cardiac hyperexcitability features manifesting as increased sinus rate, atrial ectopic rhythm and atrial and nodal tachyarrhythmias. In the current *SCN5A*-linked family, the propensity to atrial arrhythmias appeared to increase with age, resulting in paroxysmal and eventually chronic AF in many cases. Also, the number of ventricular complexes during exercise increased in some patients during follow-up, further supporting a progressive nature of the disorder. The earliest age of onset of ventricular arrhythmias among mutation carriers cannot be exactly determined using data from this single family. The youngest mutation-carrier capable of performing an exercise stress test was 11 years. Underscoring the diagnostic challenge, this boy did not exert multiple polymorphic PVCs during the clinical exercise stress test, in spite of that his 24-hour ambulatory ECG recording revealed 1210 PVCs associated with physical exercise. Even if it is clear that the p.I141V mutation is not fully penetrant, the penetrance of the PVC phenotype is high, reaching 81% when considering only adult mutation carriers.

### **Evidence for Na<sub>v</sub>1.5 p.I141V causality in exercise-induced polymorphic arrhythmias**

While sequencing two putative genes (*RYR2* and *CASQ2*) in affected members of the current family failed to identify any coding mutations, whole exome-sequencing revealed a previously unknown missense mutation in *SCN5A*, which co-segregated with the arrhythmic phenotype. The accumulated evidence strongly supports the assumption that this variant is indeed functional and causes arrhythmia in the family

investigated. First, the *SCN5A* gene resides in the only chromosomal region showing complete co-segregation with the ventricular arrhythmia phenotype. Second, the identified mutation results in an amino acid change p.I141V of the Na<sub>v</sub>1.5 protein, which *in silico* is predicted to be possibly damaging. Third, the mutation resides in a region of the *SCN5A* gene that is highly conserved between species and Na<sub>v</sub> homologues. Fourth, patch-clamp experiments show that the introduction of the mutation causes hyperexcitability of the Na<sub>v</sub>1.5 channels. Finally, computational analyses of I<sub>Na</sub> and AP in single cells imply that the biophysical changes caused by the p.I141V mutation both include an acceleration of the spontaneous depolarization rate in the Purkinje cell model, which is similar to what was reported for a MEPPC-linked p.R222Q mutation by Mann et al.<sup>2</sup>, and a reduction of the threshold for cardiac cell excitability.

Isoleucine in the position 141 of the Na<sub>v</sub>1.5 protein is highly conserved, not only across species, but also between Na<sub>v</sub> isoforms. Interestingly, Na<sub>v</sub>1.4 p.I141V and Na<sub>v</sub>1.7 p.I136V mutations, that are homologous to the Na<sub>v</sub>1.5 p.I141V mutation, have also been associated with hyperexcitability-dependent inherited disorders, i.e. with myotonia and erythromelalgia<sup>17,18,19</sup>. Both these previously described mutations induce similar modifications of the biophysical properties of the sodium voltage gated channels as was observed for the Na<sub>v</sub>1.5 p.I141V mutation in the current study<sup>17,19</sup>. Taken together, these findings strongly support the pathogenicity of this novel *SCN5A* missense variant.

### **Gain-of-function mutations in Na<sub>v</sub>1.5 and the clinical phenotypes**

Gain-of-function mutations in Na<sub>v</sub>1.5 have previously been associated with several hereditary forms of arrhythmia<sup>20</sup>, but also with the more recently described MEPPC with cardiomyopathy, that is linked to the presence of the p.R222Q mutation in Na<sub>v</sub>1.5<sup>2,3,4</sup>. In the current study the clinical phenotype, associating with the p.I141V mutation, was characterized by a distinct hyperexcitability without evidence of conduction abnormalities or QT interval prolongation. While the p.I141V and the p.R222Q mutation

both associate with atrial arrhythmias, the clinical characteristics of the individuals carrying the p.I141V mutation differ from the phenotype described in p.R222Q-carriers. Whereas exercise provoked ventricular arrhythmias in p.I141V -carriers, p.R222Q -carriers typically manifest arrhythmias at resting heart rates. Moreover, carriers of p.R222Q show frequent PVCs, with both LBBB and RBBB patterns triggered from Purkinje fibers at low heart rates, but disappearance of PVCs during exercise, and dilated cardiomyopathy<sup>2,3</sup>. In p.I141V mutation-carriers, the burden of PVCs was much lower, which may explain why they did not display any abnormalities in ventricular structure or contractility.

In spite of the above described dissimilarities between the clinical phenotypes, the differences in the cellular phenotypes associating with the p.I141V and p.R222Q mutations were more subtle. While the p.I141V mutation did not modify the voltage dependence of inactivation, it did shift the activation curve to negative potentials and led to an increase and shift of the sodium window current. In contrast, the p.R222Q mutation affects the voltage dependence of both activation and inactivation, resulting in a negative shift of the sodium window current. To bear in mind, *in vitro* phenotypes observed in heterologous expression systems may not always reflect the clinical phenotypes induced by a mutation. As an example, while many studies have reported a number of varied phenotypes associating with a *SCN5A* p.D1275N missense mutation, e.g. atrial standstill, dilated cardiomyopathy with conduction disease, atrial flutter/fibrillation, sick sinus syndrome, and ventricular dilation and dysfunction, the mutation does not induce marked  $\text{Na}_v1.5$  dysfunction *in vitro*. However, when studied in genetically engineered mice, *in vivo*, the mutation generates extensive aberration of channel function<sup>21</sup>, underscoring that functional phenotypes may be influenced substantially by the experimental systems used.

Overall, the complex pathways underlying the genotype-phenotype relationship in hereditary arrhythmia syndromes are poorly known, and the reasons for incomplete penetrance and variable expressivity remain obscure<sup>1, 22</sup>. Pleiotropy has been associated with *SCN5A* mutations in particular. While distinct clinical phenotypes have been ascribed to different mutations in the *SCN5A* gene, e.g.

LQTS, BrS and cardiomyopathy by others and the present exercise-induced phenotype by us<sup>23,24,25,26,27,28,29</sup>, some mutations also display a substantial degree of variability within families. For example, the affected family members of a large family segregating a *SCN5A*-1795insD presented with a wide array of clinical manifestations, including sinus node dysfunction, bradycardia, conduction disease, BrS, and LQTS<sup>23,24</sup>.

### **Mechanistic considerations**

The mutation-induced alterations of  $\text{Na}_v1.5$  properties and simulation studies support the concept that the increase in window current lead to a ventricular and atrial hyperexcitability. It is interesting to note that administration of flecainide 2 mg/kg i.v. to patients II-10 and III-19 resulted in a significant reduction of PVCs during an exercise stress (from 219 and 540 to 17 and 0, respectively). Also, in a previous study, flecainide has been shown to induce a dramatic reduction in PVCs and recovery of normal left ventricular function in *SCN5A* p.R222Q mutation carriers,<sup>2</sup>. While flecainide may directly act on RyR2 channels<sup>30,31,32</sup>, it has recently been suggested that the drug may reduce sodium channel availability which would increase the channel threshold for triggered activity<sup>33</sup>. Very recently, using a rat cardiomyocyte model, Sikkeli et al.<sup>34</sup> showed that flecainide reduces calcium sparks by a mechanism involving reduction of  $I_{\text{Na}}$ , i.e. through increased  $\text{Ca}^{2+}$  efflux via the sodium-calcium exchanger across the sarcolemma and reduced  $\text{Ca}^{2+}$  concentration in the vicinity of the RyR2. Given these previous observations linking  $I_{\text{Na}}$  with calcium homeostasis, one may speculate that the mechanism whereby the *SCN5A* p.I141V may cause exercise-induced PVCs in part may involve alterations of intracellular calcium flux.

### **Conclusions**

The  $\text{Na}_v1.5$  protein, encoded by the *SCN5A* gene, has previously been associated with a variety of clinical arrhythmia phenotypes, including congenital LQTS, BrS and MEPPC. The present study demonstrates that mutations in *SCN5A* also may result in exercise-induced polymorphic ventricular premature

complexes and tachycardia, hence expanding the range of phenotypes linked with variants of the *SCN5A* gene.

### **Acknowledgements**

We thank Mrs. Hanna Ranne, Minna Härkönen and Mr. Jouko Siro for their excellent technical assistance. The whole-exome sequencing, and whole-genome linkage analysis was carried out at the Technology Center at the Institute for Molecular Medicine Finland (FIMM).

### **Funding sources**

This study has been supported by grants from the Finnish Foundation for Cardiovascular Research, Helsinki, Finland, the Sigrid Juselius Foundation, Finska Läkaresällskapet, and the Swiss National Science Foundation to HA (310030 120707).

### **Disclosures**

None.

## REFERENCES

1. Wilde AA, Brugada R. Phenotypical manifestations of mutations in the genes encoding subunits of the cardiac sodium channel. *Circ Res.* 2011;108:884-897.
2. Mann SA, Castro ML, Ohanian M, Guo G, Zodgekar P, Sheu A, et al. R222Q SCN5A mutation is associated with reversible ventricular ectopy and dilated cardiomyopathy. *J Am Coll Cardiol.* 2012;60:1566-1573.
3. Laurent G, Saal S, Amarouch MY, Beziau DM, Marsman RF, Faivre L, et al. Multifocal ectopic Purkinje-related premature contractions: a new SCN5A-related cardiac channelopathy. *J Am Coll Cardiol.* 2012;60:144-156.
4. Nair K, Pekhletski R, Harris L, Care M, Morel C, Farid T, et al. Escape capture bigeminy: phenotypic marker of cardiac sodium channel voltage sensor mutation R222Q. *Heart Rhythm.* 2012;9:1681-1688 e1681.
5. Niwano S, Wakisaka Y, Niwano H, Fukaya H, Kurokawa S, Kiryu M, et al. Prognostic significance of frequent premature ventricular contractions originating from the ventricular outflow tract in patients with normal left ventricular function. *Heart.* 2009;95:1230-1237.
6. Leenhardt A, Lucet V, Denjoy I, Grau F, Ngoc DD, Coumel P. Catecholaminergic polymorphic ventricular tachycardia in children. A 7-year follow-up of 21 patients. *Circulation.* 1995;91:1512-1519.
7. Swan H, Piippo K, Viitasalo M, Heikkilä P, Paavonen T, Kainulainen K, et al. Arrhythmic disorder mapped to chromosome 1q42-q43 causes malignant polymorphic ventricular tachycardia in structurally normal hearts. *J Am Coll Cardiol.* 1999;34:2035-2042.
8. Laitinen PJ, Brown KM, Piippo K, Swan H, Devaney JM, Brahmabhatt B, et al. Mutations of the cardiac ryanodine receptor (RyR2) gene in familial polymorphic ventricular tachycardia. *Circulation.* 2001;103:485-490.
9. Swan H, Laitinen PJ. Familial polymorphic ventricular tachycardia--intracellular calcium channel disorder. *Card Electrophysiol Rev.* 2002;6:81-87.
10. Sulonen AM, Ellonen P, Almusa H, Lepistö M, Eldfors S, Hannula S, et al. Comparison of solution-based exome capture methods for next generation sequencing. *Genome Biol.* 2011;12:R94.
11. O'Connell JR, Weeks DE. PedCheck: a program for identification of genotype incompatibilities in linkage analysis. *Am J Hum Genet.* 1998;63:259-266.
12. ten Tusscher KH, Noble D, Noble PJ, Panfilov AV. A model for human ventricular tissue. *Am J Physiol Heart Circ Physiol.* 2004;286:H1573-1589.
13. Courtemanche M, Ramirez RJ, Nattel S. Ionic mechanisms underlying human atrial action potential properties: insights from a mathematical model. *Am J Physiol.* 1998;275:H301-321.
14. Stewart P, Aslanidi OV, Noble D, Noble PJ, Boyett MR, Zhang H. Mathematical models of the electrical action potential of Purkinje fibre cells. *Philos Trans A Math Phys Eng Sci.* 2009;367:2225-2255.
15. Luo CH, Rudy Y. A dynamic model of the cardiac ventricular action potential. I. Simulations of ionic currents and concentration changes. *Circ Res.* 1994;74:1071-1096.
16. ten Tusscher KH, Panfilov AV. Alternans and spiral breakup in a human ventricular tissue model. *Am J Physiol Heart Circ Physiol.* 2006;291:H1088-1100.
17. Cheng X, Dib-Hajj SD, Tyrrell L, Waxman SG. Mutation I136V alters electrophysiological properties of the Na(v)1.7 channel in a family with onset of erythromelalgia in the second decade. *Mol Pain.* 2008;4:1.
18. Lee MJ, Yu HS, Hsieh ST, Stephenson DA, Lu CJ, Yang CC. Characterization of a familial case with primary erythromelalgia from Taiwan. *J Neurol.* 2007;254:210-214.

19. Petitprez S, Tiab L, Chen L, Kappeler L, Rosler KM, Schorderet D, et al. A novel dominant mutation of the Nav1.4 alpha-subunit domain I leading to sodium channel myotonia. *Neurology*. 2008;71:1669-1675.
20. Wang Q, Shen J, Splawski I, Atkinson D, Li Z, Robinson JL, et al. SCN5A mutations associated with an inherited cardiac arrhythmia, long QT syndrome. *Cell*. 1995;80:805-811.
21. Watanabe H, Yang T, Stroud DM, Lowe JS, Harris L, Atack TC, et al. Striking In vivo phenotype of a disease-associated human SCN5A mutation producing minimal changes in vitro. *Circulation*. 2011;124:1001-1011.
22. Sturm AC, Mohler PJ. Defining the disconnect between in vitro models and human arrhythmogenic disease: context matters. *Circulation*. 2011;124:993-995.
23. Bezzina C, Veldkamp MW, van Den Berg MP, Postma AV, Rook MB, Viersma JW, et al. A single Na(+) channel mutation causing both long-QT and Brugada syndromes. *Circ Res*. 1999;85:1206-1213.
24. van den Berg MP, Wilde AA, Viersma TJW, Brouwer J, Haaksma J, van der Hout AH, et al. Possible bradycardic mode of death and successful pacemaker treatment in a large family with features of long QT syndrome type 3 and Brugada syndrome. *J Cardiovasc Electrophysiol*. 2001;12:630-636.
25. Kyndt F, Probst V, Potet F, Demolombe S, Chevallier JC, Baro I, et al. Novel SCN5A mutation leading either to isolated cardiac conduction defect or Brugada syndrome in a large French family. *Circulation*. 2001;104:3081-3086.
26. Grant AO, Carboni MP, Neplioueva V, Starmer CF, Memmi M, Napolitano C, et al. Long QT syndrome, Brugada syndrome, and conduction system disease are linked to a single sodium channel mutation. *J Clin Invest*. 2002;110:1201-1209.
27. Rossenbacker T, Carroll SJ, Liu H, Kuiperi C, de Ravel TJ, Devriendt K, et al. Novel pore mutation in SCN5A manifests as a spectrum of phenotypes ranging from atrial flutter, conduction disease, and Brugada syndrome to sudden cardiac death. *Heart Rhythm*. 2004;1:610-615.
28. Makita N, Behr E, Shimizu W, Horie M, Sunami A, Crotti L, et al. The E1784K mutation in SCN5A is associated with mixed clinical phenotype of type 3 long QT syndrome. *J Clin Invest*. 2008;118:2219-2229.
29. Nakajima S, Makiyama T, Hanazawa K, Kaitani K, Amano M, Hayama Y, et al. A novel SCN5A mutation demonstrating a variety of clinical phenotypes in familial sick sinus syndrome. *Intern Med*. 2013;52:1805-1808.
30. Watanabe H, Chopra N, Laver D, Hwang HS, Davies SS, Roach DE, et al. Flecainide prevents catecholaminergic polymorphic ventricular tachycardia in mice and humans. *Nat Med*. 2009;15:380-383.
31. Hilliard FA, Steele DS, Laver D, Yang Z, Le Marchand SJ, Chopra N, et al. Flecainide inhibits arrhythmogenic Ca<sup>2+</sup> waves by open state block of ryanodine receptor Ca<sup>2+</sup> release channels and reduction of Ca<sup>2+</sup> spark mass. *J Mol Cell Cardiol*. 2010;48:293-301.
32. Hwang HS, Hasdemir C, Laver D, Mehra D, Turhan K, Faggioni M, et al. Inhibition of cardiac Ca<sup>2+</sup> release channels (RyR2) determines efficacy of class I antiarrhythmic drugs in catecholaminergic polymorphic ventricular tachycardia. *Circ Arrhythm Electrophysiol*. 2011;4:128-135.
33. Liu N, Denegri M, Ruan Y, Avelino-Cruz JE, Perissi A, Negri S, et al. Short communication: flecainide exerts an antiarrhythmic effect in a mouse model of catecholaminergic polymorphic ventricular tachycardia by increasing the threshold for triggered activity. *Circ Res*. 2011;109:291-295.
34. Sikkell MB, Collins TP, Rowlands C, Shah M, O'Gara P, Williams AJ, et al. Flecainide reduces Ca(2+) spark and wave frequency via inhibition of the sarcolemmal sodium current. *Cardiovasc Res*. 2013;98:286-296.

**Table 1. Clinical Data of Family Members Carrying the Na<sub>v</sub>1.5 p.I141V Mutation.**

Family member #	Age 2013	Sex	Exercise-induced PVCs	Syncopal spells	Ectopic atrial rhythm	Atrial fibrillation	Threshold heart rate min <sup>-1</sup> for PVCs	Number # of PVCs during ET	Longest salvo of PVCs (beats)	Total # of PVC/ 24h	Treatment at the last follow-up visit 2013
II-2	80	F	Positive	No	+	Paroxysmal	93	231	3	1 715	Metoprolol 47.5 mg
II-4	77	M	Positive	No	-	Chronic	110	100	2	11 439	Bisoprolol 5 mg
II-7	74	M	Positive	No	+	-	90	83	4	241	Bisoprolol 2.5 mg
II-10	70	F	Positive	No	+	-	77	219	8	12 470	Propranolol 40 mg b.i.d.
II-12	65	F	Positive	No	+	Chronic	74	483	3	1 399	Amiodarone 200 mg, Bisoprolol 5 mg b.i.d.
II-14	61	F	Positive	No	-	Paroxysmal	126	630	8	5 601	Metoprolol 142.5 + 47.5 mg
III-1	61	M	Negative	No	+	-	N/A	6	1	187	None
III-3	†	M	Positive	No	-	Atrial flutter	95	492	2	N/A	Died in 2005
III-5	52	F	Positive	Yes	+	-	84	508	5	1 646	Metoprolol 47.5 mg b.i.d.
III-9	50	M	Positive	Yes	+	Chronic	108	637	5	336	Bisoprolol 7.5 mg b.i.d.
III-11	48	F	Positive	Yes	+	-	120	346	6	1 130	Bisoprolol 2.5 mg b.i.d.
III-17	37	M	Negative	No	+	-	-	1	1	3	None
III-19	34	F	Positive	No	-	-	104	540	3	9 925	None
IV-1	35	M	Positive	No	-	-	105	352	2	N/A	None
IV-3	31	M	Negative	No	-	-	N/A	4	1	N/A	None
IV-7	33	M	Positive	No	+	-	108	441	2	11	Bisoprolol 2.5mg b.i.d.
IV-13	4	M	N/A	No	-	-	N/A	N/A	N/A	4	None
IV-14	11	M	Negative	No	+	-	N/A	7	2	1 210	None
IV-15	9	F	N/A	No	-	-	N/A	N/A	N/A	4	None
V-1	2	M	N/A	No	N/A	N/A	N/A	N/A	N/A	N/A	None

PVC = premature ventricular complex, ET = exercise stress test, † = deceased, N/A = not available

**Table 2. Electrocardiographic Parameters at Rest during the Initial Evaluation in 2002-2003.**

Data are from subjects without medication.

	<b>SCN5A-positive, n=12</b>	<b>SCN5A-negative, n=17</b>	<b>p-value</b>
Age (years) (range)	42 $\pm$ 18 (21-69)	43 $\pm$ 15 (17-69)	NS
Sex (male/female)	7/5	9/8	NS
Heart rate (min <sup>-1</sup> ) (range)	79 $\pm$ 9 (63-91)	66 $\pm$ 6 (54-75)	<0.001
P (ms)	100 $\pm$ 11	100 $\pm$ 12	NS
PQ (ms)	154 $\pm$ 29	159 $\pm$ 22	NS
QRS (ms)	89 $\pm$ 15	91 $\pm$ 9	NS
QT (ms)	378 $\pm$ 35	390 $\pm$ 24	NS
QTfc (ms) (range)	413 $\pm$ 24 (383-462)	401 $\pm$ 19 (360-430)	NS

NS = not significant.

**Table 3. Formulation of the m and h Gates for the I141V Mutant  $I_{Na}$ .**

<b>LR-CRN <math>I_{Na}</math> model (16,17)</b>	<b>TNNP/SNNBZ <math>I_{Na}</math> model (15)</b>
$m_{\infty, p.I141V}(V_m) = m_{\infty, WT}(V_m - \sigma_a)$	$m_{\infty, p.I141V}(V_m) = m_{\infty, WT}(V_m - \sigma_a)$
$\tau_{m, p.I141V}(V_m) = \tau_{m, WT}(V_m - \sigma_a)$	$\tau_{m, p.I141V}(V_m) = \tau_{m, WT}(V_m - \sigma_a)$
$\beta_{h, p.I141V}(V_m) = \beta_{h, WT}(V_m - \sigma_i)$	$h_{\infty, p.I141V}(V_m) = h_{\infty, WT}(V_m)$
$\alpha_{h, p.I141V}(V_m) = \alpha_{h, WT}(V_m)$	$\beta_{h, p.I141V}(V_m) = \beta_{h, WT}(V_m - \sigma_i)$
For both genotypes:	$\alpha_{h, p.I141V}(V_m) = \alpha_{h, WT}(V_m)$
$h_{\infty}(V_m) = \alpha_h(V_m) / (\alpha_h(V_m) + \beta_h(V_m))$	For both genotypes:
$\tau_h(V_m) = 1 / (\alpha_h(V_m) + \beta_h(V_m))$	$\tau_h(V_m) = \alpha_h(V_m) / (\alpha_h(V_m) + \beta_h(V_m))$
<b>For both models:</b>	
$\sigma_a = -7 \text{ mV}$	
$\sigma_i = -7 \text{ mV}$	
$dm/dt = (m_{\infty}(V_m) - m)/\tau_m$	
$dh/dt = (h_{\infty}(V_m) - h)/\tau_h$	

WT denote the formulation of the original models. The shift parameters  $\sigma_a$  and  $\sigma_i$  were determined based on experimental data.

## FIGURE LEGENDS

### Figure 1. The Na<sub>v</sub>1.5 p.I141V Mutation

(A) The pedigree, phenotypes and mutation status of family members. The presence of  $\geq 50$  premature ventricular complexes (PVC) during an exercise stress test (ET) is indicated by a symbol with a half-filled left-side, the presence of ectopic atrial rhythm is indicated by a filled upper right quadrant and atrial fibrillation by a filled lower right quadrant. A white symbol indicated normal ECG, whereas individuals without ET are indicated with a grey symbol. The presence of the I141V mutation is specified by a + or -. (B) Targeted sequencing confirmed a heterozygous missense mutation, chr3:38,663,952 T->C, co-segregating with multiple PVCs during ET. Representative traces from four of the sequenced family-members are shown. (C) Multiple protein sequence alignments showing the conservation of isoleucine at codon 141 of the Na<sub>v</sub>1.5 protein in different vertebrate species. (D) A schematic picture of the Na<sub>v</sub>1.5 protein structure, indicating the location of the I141V-mutation in domain I.

### Figure 2. Representative ECG Registrations at Rest and During Exercise Stress Test

(A) Ectopic atrial rhythm at rest (ECG paper speed 50 mm/s) of family member III-1. (B) Ectopic atrial rhythm during early exercise (III-11, 25 mm/s). (C) Nodal rhythm during exercise (III-9, 50 mm/s). (D) First appearance of bigeminal PVCs during low work load (IV-7, 25 mm/s). (E) Multiformal PVCs and couplets during exercise (IV-7, 25 mm/s). QRS morphology vary indicating the multiple origin of PVCs. (F) Bigeminal PVCs and a short ventricular tachycardia during exercise (III-5, 25 mm/s).

### Figure 3. Experimental Effects of p.I141V Mutation on Nav1.5 Channel in HEK293 Cells

(A) Current traces obtained with a current/voltage protocol (see inset) from Na<sub>v</sub>1.5-WT and p.I141V transfected cells. Bold traces are the Na<sup>+</sup> current at -40 mV (B) Steady-state activation (WT: n=8,

p.I141V: n =9) and inactivation curves (WT: n=6, p.I141V: n =9). Activation properties were determined from I/V relationships by normalizing peak  $I_{Na}$  to driving force and maximal  $I_{Na}$ . Parameters for the voltage-dependence steady-state of activation and steady state of inactivation (20-ms test pulse to -10 mV after a 500 ms conditioning pre-pulse) are summarized in **Online Table 1**. (C) Sodium current time-to-peak values were used to evaluate the activation kinetics (WT: n=8, p.I141V: n =9). (D) Fast inactivation time constants were measured by fitting the inactivation phase of the  $Na^+$  current to a single exponential equation for WT and p.I141V (WT: n=8, p.I141V: n =9). For C and D, a two way ANOVA test followed by a Bonferroni correction was used to compare point by point the measured activation and inactivation : \*\*\*  $P < 0.001$  *versus* WT. (E) Recovery from fast inactivation was measured using the inset twin-pulse protocol (WT: n=5, p.I141V: n =7). (F) Averaged normalized WT (n=13) and p.I141V (n=14) tetrodotoxin-sensitive window currents, obtained with a 300 ms depolarizing-voltage ramp from -100 and +50 mV (0.5 mV/ms), normalized to the peak current at -20 mV recorded in the same cell. Represented in panel F are the averaged normalized window current traces at the potential range between -80 and +10 mV.

**Figure 4. Effects of the p.I141V Mutation on  $I_{Na}$  Properties, Excitability and Conduction Velocity in the Human Atrial (CRN) , the Ventricular (TNNP) and the SANNBZ Models**

(A, B, and C) Steady state activation ( $m_{\infty}^3$ ) and inactivation curves ( $h_{\infty}j_{\infty}$ ) in the CRN model (LR-CRN  $I_{Na}$  formulation) (A), the TNNP model (B), and the SANNBZ model (C). (D-F) Strength-duration curves in the CRN atrial cell model (inset: zoom on the strength-duration curves) (D), the TNNP ventricular cell model (inset: zoom of the strength-duration curves) (E), and the SANNBZ Purkinje cell model (inset: spontaneous action potentials showing the acceleration of the spontaneous rhythm due to the p.I141V mutation) (F) with WT, heterozygous (Het) and homozygous p.I141V genotypes (pacing rate 1 Hz and/or 2.5 Hz). (G-I) Excitation thresholds at 2 ms stimulus duration in the CRN atrial AP model (G), the TNNP ventricular AP model (H), and the SANNBZ Purkinje AP model (I) (pacing rate 1 Hz and/or 2.5 Hz). (J-

**L)** Conduction velocities in the atrial CRN model (**J**), the ventricular TNNP model (**K**) and the SANNBZ Purkinje model (**L**) (pacing rate 1 Hz and / or 2.5 Hz). Strength-duration curves and conduction velocities could not be established at 1 Hz in the Purkinje model because of the accelerated spontaneous rhythm caused by the p.I141V mutation.

Fig.1

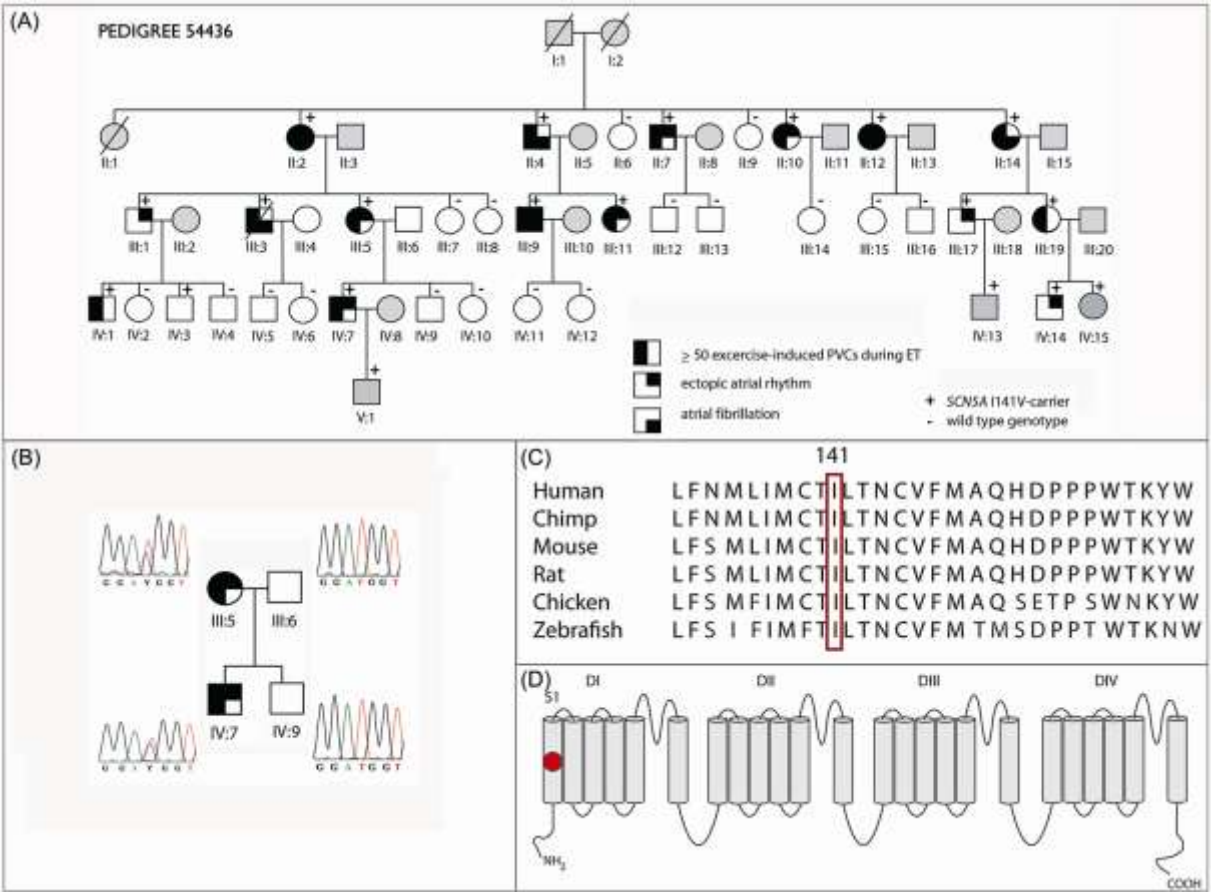


Fig.2

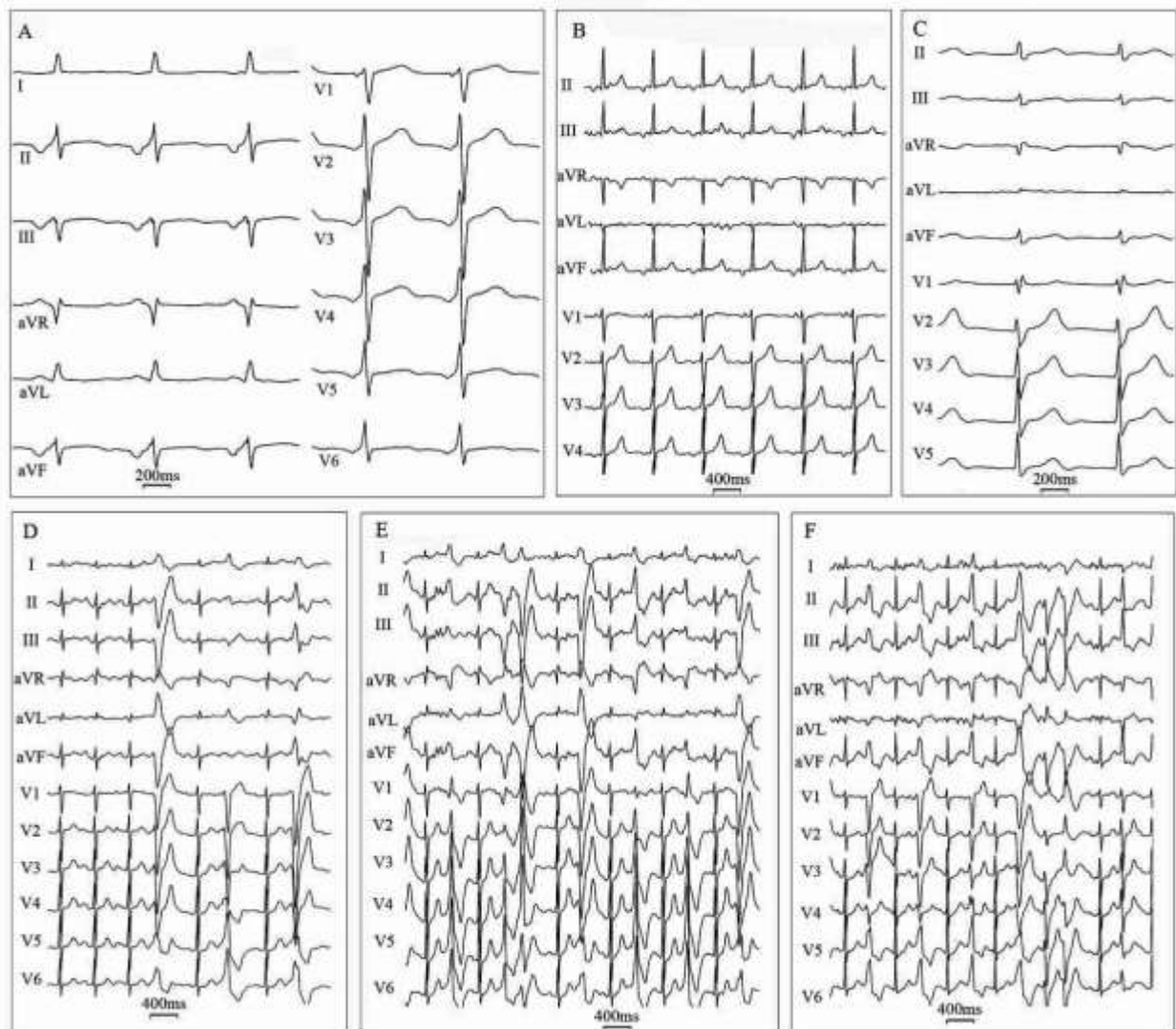


Fig. 3

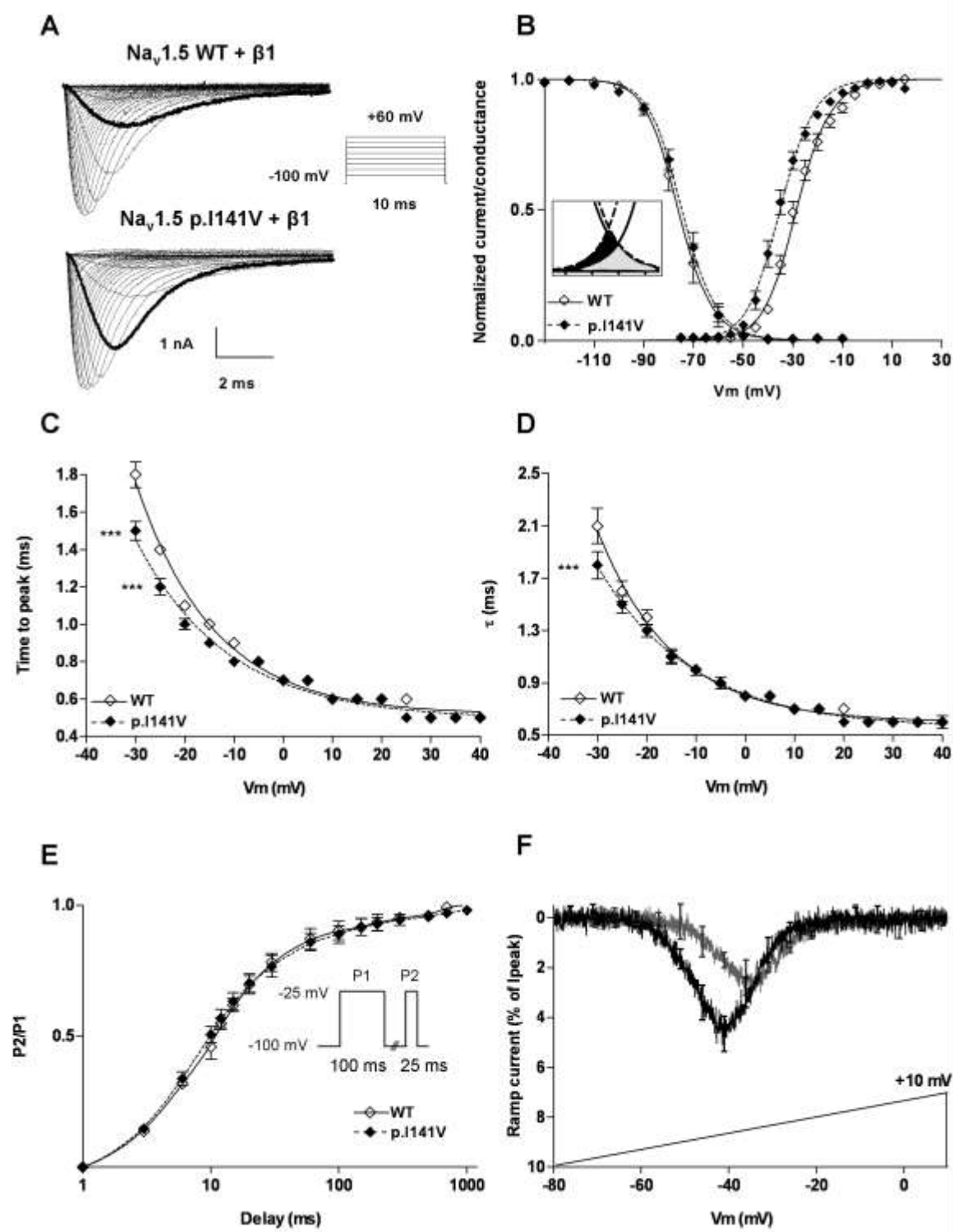


Fig.4

